HHS Public Access

Author manuscript

Cancer Immunol Res. Author manuscript; available in PMC 2018 October 26.

Published in final edited form as:

Cancer Immunol Res. 2018 April ; 6(4): 434–447. doi:10.1158/2326-6066.CIR-17-0345.

Macrophages and CD8+ T cells mediate the antitumor efficacy of combined CD40 ligation and imatinib therapy in gastrointestinal stromal tumors

Jennifer Q. Zhang[1], **Shan Zeng**[1], **Gerardo A. Vitiello**[1], **Adrian M. Seifert**[1], **Benjamin D. Medina**[1], **Michael J. Beckman**[1], **Jennifer K. Loo**[1], **Juan Santamaria-Barria**[1], **Joanna H. Maltbaek**[1], **Nesteene J. Param**[1], **John A. Moral**[1], **Julia N. Zhao**[1], **Vinod Balachandran**[1], **Ferdinand Rossi**[1], **Cristina R. Antonescu**[2], and **Ronald P. DeMatteo**[1,3]

[1]Department of Surgery, Memorial Sloan Kettering Cancer Center, New York, NY

[2]Department of Pathology, Memorial Sloan Kettering Cancer Center, New York, NY

[3]Department of Surgery, Hospital of the University of Pennsylvania, Philadelphia, PA

Abstract

Tyrosine kinase inhibition of gastrointestinal stromal tumors (GIST) is effective but typically culminates in resistance and is rarely curative. Immunotherapy has potential application to GIST, as we previously showed that T-cell checkpoint blockade increases the antitumor effects of imatinib. Here, we showed that ligation of CD40 using an agonistic antibody (anti-CD40) activated tumor-associated macrophages (TAMs) *in vivo* in a knock-in mouse model of GIST harboring a germline mutation in *Kit* exon 11. Activated TAMs had greater TNF production and NFκB signaling and directly inhibited tumor cells *in vitro*. Anti-CD40 required concomitant therapy with imatinib for efficacy and depended on TAMs, and to a lesser extent $CD8^+$ T cells, but not on $CD4^+$ T cells or B cells. In an analysis of 50 human GIST specimens by flow cytometry, we found that CD40 was expressed on human TAMs and tumor cells yet was downregulated after response to imatinib. CD40 ligation did not have a direct inhibitory effect on human GIST cells. Our findings provide the rationale for combining anti-CD40 and tyrosine kinase inhibition to treat human GIST.

Keywords

Gastrointestinal stromal tumor; CD40; tumor-associated macrophage; immunotherapy

Introduction

Gastrointestinal stromal tumors (GISTs) are the most common type of sarcomas and occur primarily in the stomach and small bowel, followed by other parts of the gastrointestinal tract (1). Approximately 75% of GISTs contain an activating mutation in *KIT*, whereas 10%

Corresponding author: Ronald P. DeMatteo, Hospital of the University of Pennsylvania, Philadelphia, PA 19104, Phone: 215-662-7539, Fax: 215-614-0363, ronald.dematteo@uphs.upenn.edu.

Disclosures: The authors have no financial conflict of interest.

have a platelet-derived growth factor receptor α (*PDGFRA*) mutation (2, 3). The advent of tyrosine kinase inhibitors such as imatinib mesylate, which effectively targets both KIT and PDGFRα, has revolutionized the treatment of GISTs (1, 4, 5). However, imatinib is rarely curative and resistance frequently develops within two years (5, 6). Sunitinib and regorafenib are the second and third line inhibitors after imatinib failure, but these tyrosine kinase inhibitors usually fail within a few months (7, 8). Therefore, novel therapeutic strategies in addition to tyrosine kinase inhibition are needed.

Although GISTs are primarily defined by an activating mutation in *KIT or PDGFRA*, substantial evidence that the immune environment plays a critical role in modulating tumor growth exists. Both T cells and tumor associated-macrophages (TAMs) are important in the maintenance of the tumor microenvironment and are altered by treatment with imatinib, as we have previously shown (9-11). In particular, GIST TAMs become M2-like (i.e., pro-tumoral and less activated) with imatinib therapy (10). We, therefore, sought a strategy to further activate TAMs through CD40 ligation. CD40 is a member of the tumor necrosis factor receptor family and is mainly expressed on antigen presenting cells (APCs) including macrophages, monocytes, dendritic cells, and B cells, as well as a variety of non-immune cells (12-14). Under normal conditions, CD40 ligand (CD40L, CD154) on activated T-helper cells interacts with APCs via CD40, resulting in $CD8^+$ T cell activation (15). CD40 agonism in tumor models has been shown to depend upon $CD8^+$ T cells (16-18), macrophages (19), and B cells (20). Even tumor cells can express CD40 on their cell surface and can undergo apoptosis or growth inhibition after CD40 ligation (21-23). Multiple agonistic CD40 antibodies have been developed for clinical use and responses in melanoma and pancreas cancer have been reported (24).

In this study, we discovered that the combination of anti-CD40 and imatinib was effective in a preclinical model of GIST, and the mechanism depended on macrophages and partly on $CD8^+$ T cells. We also identified CD40 expression in human GIST TAMs and tumor cells. Our studies support that TAMs may be manipulated for therapeutic benefit in human GIST.

Materials and Methods

Mice and treatments.

Age- and sex-matched 8-16 week old $Kit^{V558\Delta/+}$ mice (25), $Kit^{V558\Delta;T669I/+}$ mice (26), and NOD.Cg-*Prkdc*^{scdi}*Il2rg*^{tm1Wjl}/SzJ (NSG) mice (Jackson Laboratory) were used in accordance with an Institutional Animal Care and Use Committee protocol. Tumors in $Kit^{V558\Delta/+}$ mice were established by 8 weeks of age. The treatment antibodies listed below were obtained from Bio X Cell unless otherwise indicated. $Kit^{V558\Delta/+}$ mice received one dose of an agonistic CD40 antibody (clone FGK4.5, 100 μg intraperitoneal [i.p.]) or rat IgG2a (clone 2A3, 100 μg i.p.) on day 0, which indicates first day of treatment. Imatinib (600 mg/L in drinking water; Novartis) was started on day 3 and continued until the end of the experiment, unless otherwise indicated. Anti-CSF1R (clone AFS98) or Rat IgG2a (clone 2A3) was given on day 0 (500 μg i.p.) and days −7, −5, −3, 1, 4, 8, and 11 (250 μg i.p.). Anti-CD4 (clone GK1.5, 400 μg i.p.) or rat IgG2b (clone LTF-2, 400 μg i.p.) was given on days −3, −2, −1, 4, and 11 for $CD4^+$ T-cell depletion. Anti-CD8 (clone 2.43, 250 μg i.p.) or rat IgG2b (clone LTF-2, 250 μg i.p.) was given on days −3, −2, −1, 5, and 12 for $CD8^+$ T-

cell depletion. Anti-IFNγ (clone XMG1.2, 500 μg i.p.) or rat IgG1 (clone HRPN, 500 μg i.p.) was given on days −2 and −1, then 250 μg i.p. on days 0, 2, 5, 8, 11, and 13. Anti-CD20 (clone 18B12, 250 μg i.p., obtained from Biogen) or mouse IgG2a (clone C1.18.4, 250 μg i.p.) was given on days −14 and 0 for B-cell depletion. PLX5622 (1200 mg/kg chow; provided by Plexxikon) or control chow AIN-76A (Plexxikon) were started on day −7 and continued for the duration of the experiment. Clodronate liposomes (clodronateliposomes.org; 10 μg/gram mouse body weight i.p.) were given on day −3 and every 4-5 days thereafter.

For xenograft experiments, GIST T1 cells (1×10^6) in PBS mixed 1:1 with BD Matrigel Matrix Growth Factor Reduced (BD Biosciences) were injected subcutaneously into flanks of NSG mice, (5-6 mice per group) as previously described (27), and treated with IgG (Bio X Cell), anti-human CD40 (clone G28.5, 100 μg i.p.; Bio X Cell), IgG and imatinib, or anti-human CD40 and imatinib. Anti-human CD40 or IgG were given on day 0 and imatinib or control water started on day 3 and continued until the end of the experiment. The human GIST-T1 cell line (provided by Dr. Takahiro Taguchi, Kochi Medical School) underwent confirmation of Kit expression and mutation status by Western blot and sequencing. Cells were stored in 10% DMSO in liquid nitrogen and used within one month of thawing. Cells were cultured in RPMI 1640 medium containing 10% FCS. Mycoplasma testing was performed prior to use.

Flow cytometry.

Flow cytometry was performed using a FACSAria (BD) and LSRFortessa (BD). Tumors and spleens from $Kit^{V558\Delta/+}$ and $Kit^{V558\Delta;T669I/+}$ mice were processed as previously described (11). After mincing, tumors were incubated in 5 mg/mL collagenase IV (Sigma-Aldrich) and DNAse I (0.5 mg/mL, Roche Diagostics) in HBSS for 30 minutes while shaking at 37°C. Spleens were mashed through a 70 micron filter and RBC lysis was performed using RBC lysis buffer (eBioscience). Bone marrow was harvested from the femur, resuspended in PBS, and filtered through a 40 micron filter. Single-cell suspensions were stained using antibody cocktail in 100uL of PBS + 5% fetal bovine serum in the dark at 4°C, washed, and analyzed immediately by flow cytometry. Mouse-specific antibodies conjugated to various fluorochromes were purchased: from Biolegend - CD45 (Clone 30-F11), PD1 (Clone 29F. 1A12), F4/80 (Clone BM8), CCR2 (Clone SA203G11); from BD Biosciences - CD45 (Clone 30-F11), CD69 (Clone H1.2F3), CD11c (Clone HL3), MHCII (Clone M5/114.15.2), CD117 (Clone 2B8), CD40 (Clone HM40-3), Ly6C (Clone, AL-21), CD3 (Clone 145-2C11), CD11b (Clone MI/70), CD4 (Clone RM4-5), CD4 (Clone GK1.5), CD80 (Clone 16-10A1), CD86 (Clone GL1); from Invitrogen - F4/80 (Clone BM8), Granzyme B (Clone GB11), and from eBioscience - MHCII (Clone M5/114.15.2), CD8 (Clone 53-6.7), F4/80 (Clone BM8), CD19 (Clone 1D3), CD117 (Clone ACK2).

Human-specific antibodies conjugated to various fluorochromes were purchased: from Biolegend - CD4 (Clone HB14), CD40L (Clone 24-31); from BD Biosciences - CD3 (CloneSK7), CD56 (Clone B159), CD45 (Clone 2D1), CD19 (Clone HIB19), CD14 (Clone M5E2), CD11b (Clone D12), CD117 (Clone 104D2), and from eBioscience - CD66b (Clone G10F5). Cell culture supernatants were measured at three days using a cytometric bead array

(Mouse Inflammation Kit; BD Biosciences), as instructed. Annexin V staining was performed using the eBioscience Annexin V staining kit, as directed. TAMs were sorted using a viability dye, CD45, F4/80, and CD11b, using the Flow Cytometry Core Facility's FACSAria. Purity was >90% by flow cytometry.

Cell isolation.

Single-cell suspensions of tumors were incubated with anti-mouse F4/80 microbeads (Miltenyi Biotec) and passed through two sequential LS columns per 3×10^7 cells, saving the final $F4/80^+$ fraction, as per the manufacturer's protocol, and were used immediately in cell culture experiments or pelleted, flash frozen, and stored at −80°C for use in subsequent mRNA analysis and western blotting. Kit^+ tumor cell selection was performed by incubating single-cell suspensions of tumor cells with anti-human CD45 microbeads (Miltenyi Biotec) and collecting the negative fraction. The $CD45^-$ fraction was then incubated with CD117 microbeads (Miltenyi Biotec), and the positive fraction was collected. Cells were pelleted, flash frozen, and stored at −80°C for use in subsequent western blotting. Purity was >90% by flow cytometry.

Cell assays and treatments.

TAMs used in coculture experiments were bead-isolated from *in vivo* treated (IgG, anti-CD40, IgG and imatinib, anti-CD40 and imatinib) $Kit^{V558\Delta/+}$ tumors. The murine S2 GIST cell line was derived in our laboratory from an untreated $Kit^{V558\Delta/+}$ tumor (10). Kit mutation status was confirmed by sequencing. Cells were stored in 10% DMSO in liquid nitrogen and used within one month of thawing. Cells were cultured in RPMI 1640 medium containing 10% FCS. Mycloplasma testing was performed prior to use. Using 96-well round bottom plates, 4×10^4 TAMs were cocultured with 1×10^3 S2 cells using RPMI 1640 medium containing 10% FCS for 3 days. Cell viability assays were performed in 96-well plates using Cell Counting Kit-8 (Dojindo), according to the manufacturer's protocol. Human GIST T1 (28) and HG129 (27) (*KIT* exon 11 mutation), and GIST882 (*KIT* exon 13 mutation, provided by Jonathan Fletcher) were maintained in RPMI-1640 media and 10% FCS as previously described (11).

4×10^6 GIST-T1 cells were treated with imatinib (100 nM; Novartis), recombinant human IFNγ (100 ng/mL; R&D Systems), recombinant human TGFβ (10 ng/mL; R&D Systems), recombinant human TNFα (10 ng/mL; R&D Systems).

Quantitative real-time PCR.

Total RNA was extracted from tumor tissues or cells, reverse transcribed using TaqMan Reverse Transcription Agents, and amplified (singleplex) using 20ng cDNA in duplicate with PCR TaqMan probes for murine *CD40* (Mm00441891_m1), *CCL2* (Mm00441242_m1), *IFNG* (Mm01168134_m1), *TNF* (Mm00443258_m1), *TGFB* (Mm01178820_m1), *IL6* (Mm00446191_m1), *IL10* (Mm00439616_m1), and *GAPDH* (Applied Biosystems, commercially available full gene expression assays); and human *TNF* (Hs00174128_m1), *IFNG* (Hs00989291_m1), *TGFB* (Hs00998133_m1), and *CD40* (Hs01002915_g1). Quantitative PCR was performed using a ViiA™7 real-time PCR system (Applied Biosystems, commercially available full gene expression assays). Data were

calculated by the $2^{-\Delta\Delta Ct}$ method as described in the manufacturer's instructions and expressed as fold increase over control.

Western blot.

Protein from snap frozen tissues was isolated as before (25). In brief, snap frozen tumor tissue was homonized in a PowerGen 10000 homogenizer (Thermo Fisher Scientific) in lysis buffer and incubated for 30 minutes on ice. Lysates were cleared by centrifugation at 4°C for 10 minutes. Protein from cell pellets was isolated by pipetting in NP-40 cell lysis buffer (Life Technologies) containing 1% PMSF, incubating on ice for 30 minutes, and removing cleared lysate after centrifugation. Antibodies were purchased from Cell Signaling Technology- phospho-KIT Y719, KIT (Clone D13A2), phospho-AKT Ser473, AKT (Clone 11E7), phospho-ERK T202/Y204, ERK1/2, phospho-4EBP1 S65, phospho-NFκB p65 Ser536, GAPDH, and from Santa Cruz - CD40 (Polyclonal C-20).

Immunohistochemistry.

Immunohistochemistry (IHC) was performed as before (11). Ki67 (Vector Laboratories) and CD40 (Polyclonal C-20; Santa Cruz) staining of mouse and human tissues, respectively, was performed by the institutional Molecular Cytology Core. Slides were either imaged on an Axio wide-field microscope (Zeiss) or scanned with MIRAX scan (Zeiss) and analyzed with Pannoramic Viewer by laboratory member. Ki67 was quantified by manually counting stained nuclei in the field size, as indicated. Trichrome staining was quantified using ImageJ software's Colour Deconvolution Plug-In (29).

Patient Samples.

Fifty tumor samples were obtained from 43 patients with GIST who underwent surgery at our institution and written consent was given for participation in an Institutional Review Board-approved protocol. Tumors were all GISTs by pathology with at least 0.5 grams of tissue available for analysis. Samples were sent directly from the operating room to the tissue procurement service, where they were sectioned for pathology as well as for research. Samples were stored at 4°C and processed within 2 hours of removal. Human tumor tissue was processed in the same manner as murine tumors described above. Mitotic rate was gathered from surgical pathology reports. Paraffin-embedded tumor and adjacent lymph node were stained for CD40 as stated above.

Statistical analysis.

Unpaired, two-tailed Student *t* test was performed on datasets using Graph Pad Prism 6.0 (Graph Pad Software). A P value < 0.05 was considered significant. Data are shown as mean ± SEM or median. Spearman correlation was performed where applicable.

Results

Anti-CD40 activates TAMs and recruits inflammatory monocytes

In order to investigate the effects of anti-CD40 in murine GIST, we used $Kit^{V558\Delta/+}$ mice, containing a mutation in exon 11 of *Kit*, the most frequently affected site in human GIST.

The mice develop a single, non-metastatic GIST in the cecum with 100% penetrance (25). Previously, we showed in $Kit^{V558\Delta/+}$ mice and human GISTs that TAMs are inflammatory and antitumoral (M1-like) at baseline but become less inflammatory (M2-like) after imatinib therapy (10). However, no therapeutic advantage to depleting TAMs during imatinib therapy in $Kit^{V558\Delta/+}$ mice was seen (10). Therefore, we sought to activate TAMs using an agonistic CD40 antibody (anti-CD40) to improve imatinib's antitumor effects. In $Kit^{V558\Delta/+}$ mice, CD40 was expressed on subsets of APCs within the tumor and spleen, including macrophages, monocytes, dendritic cells (DCs), and B cells (Fig. 1A-B). TAMs were defined as $CD45^+Ly6G^-CD11b^+F4/80^+Ly6C^{lo}$, whereas monocytes were defined as $CD45^+Ly6G^-CD11b^+F4/80^+Ly6C^{hi}$ (Supplementary Fig. S1A) (30). Dendritic cells were defined as $CD45^+F4/80^-CD11c^+MHCII^+$ (Supplementary Fig. S1B), and B cells as $CD45^+CD3^-CD19^+$. Within the tumor, monocytes and TAMs had the highest percentage of CD40 staining (Fig. 1A-B). Neutrophils ($CD45^+CD11b^+Ly6G^+$) (Supplementary Fig. S1A) and myeloid-derived suppressor cells (MDSCs, $CD45^+F4/80^-CD11b^+$ and $Ly6G^+$ or $Ly6C^+$) (Supplementary Fig. S1B) represented less than 1% of intratumoral immune cells. DCs and MDSCs were not altered by treatment (Fig. S1C). Three days after a single injection of anti-CD40 in $Kit^{V558\Delta/+}$ mice, monocytes increased within the tumor, whereas TAMs, as a percentage of $CD45^+$ cells, remained stable (Fig. 1C). The infiltrating monocytes were more inflammatory, expressing higher CD11c, CD80, and CD40 (Fig. 1D). TAMs upregulated the activation markers CD80 and CD40, whereas CD11c increased slightly but was already high at baseline, as was MHCII, consistent with their M1-like properties (Fig. 1D) (10). One day after anti-CD40 injection, the percentage of monocytes ($Ly6C^+CD11b^+$) in the bone marrow was reduced (Fig. 1E), yet they had increased activation markers (Fig. 1F). A large increase in the production of CCL2, a monocyte chemoattractant, was seen within the tumor (Fig. 1G). Combined, these data suggested that anti-CD40 not only activated TAMs *in vivo*, but also rapidly mobilized activated monocytes from the bone marrow into the tumor.

CD40 ligation increases the antitumoral effects of imatinib

Given our findings that anti-CD40 could activate and attract inflammatory myeloid cells, we hypothesized that anti-CD40 therapy would increase the antitumor effects of imatinib. We treated $Kit^{V558\Delta/+}$ mice, that had established tumors, with a single dose of anti-CD40 or control IgG on day 0, followed by continuous imatinib or vehicle starting on day 3, and then tumors were analyzed at 2 weeks (Fig. 2A). $Kit^{V558\Delta/+}$ mice have reproducible tumor sizes based on age and sex, allowing the use of tumor weight as a marker of efficacy(9). The combination of anti-CD40 and imatinib decreased tumor weight and size compared to imatinib alone (Fig. 2B, C). The effect was more pronounced, with decreased cellularity with H&E staining, increased collagen deposition seen with trichrome staining, and decreased proliferation indicated by Ki67 staining (Fig. 2D, E). Imatinib alone did not produce a histologic effect by H&E in $Kit^{V558\Delta/+}$ mice, despite drastically decreasing tumor weight and generating a moderate Trichrome response, as we have observed previously (31). Consistent with these findings, the combination of anti-CD40 and imatinib further decreased the percentage of Kit^+ tumor cells and the amount of Kit protein per tumor cell, as assessed by flow cytometry (Fig. 2F, G). Western blots showed that anti-CD40 and imatinib decreased p-KIT and the downstream pathway mediators p-AKT and p-ERK (Fig. 2H).

Collectively, our findings highlighted the importance of the CD40-CD40L axis in GIST and demonstrated the antitumor efficacy of anti-CD40 when combined with imatinib.

Anti-CD40 combination therapy is macrophage-dependent

To determine the mechanism of the antitumor effects of anti-CD40 and imatinib, we tested the effect of TAM depletion. We have previously showed that TAMs can be depleted in $Kit^{V558\Delta/+}$ mice by inhibiting CSF1R with either the blocking antibody AFS98 or the small molecule CSF1R inhibitor PLX5622 (10). However, neither PLX5622 or anti-CSF1R (AFS98) administration during combined anti-CD40 and imatinib therapy depleted TAMs (Fig. 3A, Supplementary S2A), likely owing to monocyte recruitment resulting from CD40 ligation. Anti-CD40 and imatinib in combination with either PLX5622 or αCSF1R resulted in an $F4/80^{hi}$ and $F4/80^{lo}$ TAM population (Fig. 3B, Supplementary S2B). The $F4/80^{hi}$ TAMs were higher in Ly6C, MHCII, and CD11c expression compared to $F4/80^{lo}$ TAMs in mice treated with combination anti-CD40, imatinib, and PLX5622 (Fig. 3C). We, therefore, attempted to block the recruitment of new TAMs from the periphery during anti-CD40 and imatinib therapy. The addition of clodronate liposomes (32) to the CSF1R inhibitor PLX5622 successfully depleted TAMs (Fig. 3D). TAM depletion abrogated the efficacy of combined anti-CD40 and imatinib therapy based on tumor weight, percentage of Kit^{+} tumor cells, collagen density by Trichrome, Ki67 by IHC, H&E, and KIT signaling (Fig. 3D-F). TAM depletion in the setting of anti-CD40 and imatinib therapy did not alter the numbers of DCs and monocytes as a percentage of $CD45^{+}$ cells (Supplementary Fig. S3).

We next sought to determine whether anti-CD40–activated TAMs could directly inhibit tumor cell growth. $Kit^{V558\Delta/+}$ mice treated with anti-CD40 and imatinib were sacrificed four days later after treatment start, and TAMs were isolated and cocultured with murine GIST S2 cells derived from a $Kit^{V558\Delta/+}$ tumor (10). S2 cells cocultured with TAMs from mice treated with anti-CD40 alone or anti-CD40 plus imatinib had lower viability (Fig. 3G) and greater apoptosis by Annexin V staining (Fig. 3H). TAMs from mice treated with anti-CD40 alone or anti-CD40 plus imatinib also produced more TNF and IL6 when cultured alone or with S2 cells (Fig. 3I). CD40 engagement can activate a number of downstream pathways, including NFκB, PI3K, and MAPK (33). TAMs from $Kit^{V558\Delta/+}$ mice treated with anti-CD40 in combination with imatinib exhibited increased phosphorylation of NFκB p65 but demonstrated no change in the PI3K pathway mediator p-4EBP1 or MAPK pathway (Fig. 3J). This indicated that anti-CD40–induced changes in GIST TAMs were partially mediated through the NFκB pathway, a known inducer of multiple inflammatory cytokines (34, 35). Increased production of TNF and IL6 production, along with decreased IL10 production, in TAMs was observed after two weeks of therapy in $Kit^{V558\Delta/+}$ mice (Fig. 3K), suggesting that the TAMs became more functionally M1 with combination therapy. Thus, TAMs were essential for the antitumor activity of anti-CD40 and imatinib.

KIT inhibition and sequence of therapy may be important for tumor response.

Because anti-CD40 alone activated TAMs but did not induce antitumor effects, we sought to determine whether the addition of imatinib was necessary because of its ability to inhibit KIT or whether it was due to some other off-target effect. $Kit^{V558\Delta;T669I/+}$ mice are imatinib-resistant, due to the inability of imatinib to bind to the doubly mutated protein, and develop

cecal GISTs that are fivefold smaller than GISTs of $Kit^{V558\Delta/+}$ mice (26). At baseline, more monocytes and fewer TAMs were present in $Kit^{V558\Delta;T669I/+}$ tumors **(Fig. 4A)**. However, the tumors of $Kit^{V558\Delta;T669I/+}$ mice responded similarly to anti-CD40 at three days, with increased intratumoral monocytes and CD11c, CD80, and CD40 expression on TAMs (Fig. 4B and C). The combination of anti-CD40 and imatinib did not have an antitumor effect in imatinib-resistant $Kit^{V558\Delta;T669I/+}$ mice, as measured by Ki67 and H&E (Fig. 4D and E). The small size of $Kit^{V558\Delta;T669I/+}$ tumors precluded using weight as an indicator of antitumor efficacy. These data suggested that KIT inhibition was necessary for the combination of anti-CD40 and imatinib to be effective.

Because imatinib can sometimes suppress the immune system by decreasing IFNγ, inhibiting dendritic cells, and modulating TAMs from M1 to M2 (10, 11, 36), we hypothesized that giving imatinib first may diminish the efficacy of combination therapy. Administration of imatinib followed by anti-CD40 three days later failed to decrease tumor weight and Ki67 IHC count at two weeks (Supplementary Fig. S3A and B), and the histologic effect was reduced (Supplementary Fig. S3C). TAMs isolated from $Kit^{V558\Delta/+}$ mice treated with imatinib followed by anti-CD40 did not have increased TNF and IL6 production when cultured alone or with S2 cells (Supplementary Fig. S3D), unlike TAMs isolated from $Kit^{V558\Delta/+}$ mice treated with anti-CD40 first (Fig. 3H). Taken together, these data indicated the importance of administering anti-CD40 first for an optimal tumor response.

Anti-CD40 combination therapy partially depends on $CD8^+$ T cells

Because many prior studies have shown the importance of T cells in the context of anti-CD40 cancer therapy, we investigated the role of T cells in $Kit^{V558\Delta/+}$ mice treated with anti-CD40. Three days after injection of anti-CD40 alone in $Kit^{V558\Delta/+}$ mice, intratumoral and splenic $CD4^+$ and $CD8^+$ T cells were activated, with upregulation of CD69, granzyme B, and PD-1 (Fig. 5A). After two weeks of therapy, the addition of anti-CD40 did not change $CD3^+$ T cells as a percentage of $CD45^+$ cells (Fig. 5B) or $CD45^+$ cells as percentage of total cells (Supplementary Fig. S5). After depletion of $CD8^+$ T cells, anti-CD40 plus imatinib still decreased the percentage of Kit^+ tumor cells and induced histologic changes compared to imatinib alone, but less reduction in tumor weight, less collagen accumulation, and less effect on Ki67 staining was seen (Fig 5C and D). Conversely, $CD4^+$ T-cell depletion during combined anti-CD40 and imatinib therapy did not affect the changes in tumor weight, percentage of Kit^+ tumor cells, collagen (Trichrome), Ki67 staining, or cellularity by H&E (Fig. 5D and E). B cells, which expressed CD40 (Fig. 1A and B), did not contribute to the antitumor effect (Fig. 5D and F). Taken together, these studies indicated that the effects of combined anti-CD40 and imatinib partially depended on $CD8^+$ T cells but were independent of $CD4^+$ T cells and B cells.

CD40 ligation does not directly inhibit GIST cells.

We found that CD40 was also expressed on some tumor cells from $Kit^{V558\Delta/+}$ mice (Fig. 6A)at a similar frequency as on TAMs (Fig. 6B). Imatinib therapy for two weeks downregulated CD40 expression on Kit^+ tumor cells from $Kit^{V558\Delta/+}$ mice, whereas anti-CD40 increased it (Fig. 6C). CD40 was also expressed on the surface of the human GIST

cell lines GIST T1, GIST 882, and HG129 (Fig. 6D). Imatinib did not decrease CD40 expression on GIST T1 cells *in vitro* (Fig. 6E). CD40 expression on GIST T1 cells was increased by IFNγ, and to a lesser extent TNF and TGFβ (Fig. 6F). Because imatinib decreased tumor IFNγ, TNF, and TGFβ in $Kit^{V558\Delta/+}$ tumors (Fig. 6G), CD40 downregulation in Kit^{+} tumor cells may be due to the indirect effect of imatinib on these cytokines. To assess whether anti-CD40 had a direct inhibitory effect on tumor cells *in vivo*, we treated established GIST T1 xenografts with human anti-CD40. No significant antitumor effects were observed (Fig. 6H). Thus, anti-CD40 did not directly inhibit human GIST cells.

CD40 is expressed in human GISTs and correlates with treatment status

To ascertain the clinical relevance of some of our mouse findings, we analyzed CD40 expression in 50 GISTs from 43 patients (Supplementary Table S1). Diffuse expression by immunohistochemistry was seen (Fig. 7A). CD40 was expressed on TAMs (Fig. 7B) and freshly-isolated Kit^{+} tumor cells (Fig. 7C and D), but a wide variation in expression was found (Fig. 7E). CD40 expression on Kit^{+} tumor cells and TAMs was lower in sensitive (i.e., responding to imatinib) tumors compared to untreated or resistant tumors but, otherwise, did not correlate with location, mutation, or mitotic rate (Fig. 7F), which are markers of tumor biology in human GIST. Within individual tumors specimens, no strong correlation of CD40 expression between tumor cells and TAMs was found (Fig. 7G). Among multiple tumors from the same patient, tumor cells had similar CD40 staining, as did TAMs (Fig. 7H). CD40L expression was also present and highest in intratumoral $CD4^{+}$ T cells (Fig. 7I). The presence of CD40 expression in human GISTs supports the possibility that CD40-based therapy may be effective in human GIST.

Discussion

Agonistic CD40 therapy further inhibited tumor growth in $Kit^{V558\Delta/+}$ GIST-bearing mice when combined with imatinib, and the mechanism depended largely on macrophages and less on $CD8^{+}$ T cells. Previously, we reported that TAMs in $Kit^{V558\Delta/+}$ tumors and human GISTs are M1-like at baseline, as they expressed activation markers, stimulated T cells, and secreted pro-inflammatory cytokines (10). Four weeks of TAM depletion with the small molecule CSF1R inhibitor PLX5622 increased tumor weight in $Kit^{V558\Delta/+}$ mice. Imatinib therapy in both $Kit^{V558\Delta/+}$ mice and GIST patients polarized TAMs to a more M2-like phenotype. Nevertheless, TAM depletion in the setting of imatinib therapy did not further reduce tumor weight in $Kit^{V558\Delta/+}$ mice(10). Therefore, we sought alternative approaches to manipulate TAMs for therapeutic advantage during imatinib therapy. Anti-CD40 therapy activated TAMs and recruited inflammatory monocytes into the tumor microenvironment. TAMs from $Kit^{V558\Delta/+}$ mice treated with anti-CD40 and imatinib produced more inflammatory cytokines and achieved greater direct tumor inhibition *in vitro*. Even after two weeks of treatment, the activated TAMs were more M1-like and continued to produce increased TNF and IL6 compared to TAMs from mice treated with imatinib alone. Murine GISTs increased CCL2 production after CD40 ligation, likely contributing to the recruitment of inflammatory monocytes to the tumor from the bone marrow and amplification of the antitumor response. We demonstrated that TAM depletion abrogated the tumor weight and histologic effects of anti-CD40 and imatinib therapy.

The effects of anti-CD40 in many other tumor models have relied on $CD8^+$ T cells (16–18). In our GIST model, we found that $CD8^+$ T cells appeared to play a partial role in the anti-CD40 and imatinib effect. Combination therapy during $CD8^+$ T-cell depletion achieved only a small decrease in tumor weight, yet a moderate decrease in Ki67 staining and a moderate increase in collagen was observed. Thus, the predominant mechanism of combined anti-CD40 and imatinib appeared to be through TAMs. We found that treatment with anti-CD40 upregulated PD-1. Just as CD40 has been cited as a resistance mechanism to PD-1/PDL-1 blockade (37, 38), the PD-1/PDL-1 axis has also been implicated in resistance to anti-CD40 (39). It is conceivable that anti–PD-1 therapy may ameliorate T-cell exhaustion induced by anti-CD40 and enable sustained T-cell activation in the setting of macrophage activation.

The mechanism of combined CD40 ligation and imatinib, therefore, was mediated predominantly by activated intratumoral TAMs and partly by $CD8^+$ T cells. The resulting tumor cell loss and reduction in proliferation were accompanied by a decrease in KIT signaling, which we have observed previously after extensive tumor destruction, such as after treatment with crizotinib (a MET inhibitor) and imatinib (27). Although tumor cells expressed CD40 in our mouse model and in human GIST specimens, anti-CD40 did not have a direct inhibitory effect on tumor growth in GIST T1 xenografts.

It is important to recognize that although imatinib decreases tumor weight in $Kit^{V558\Delta/+}$ mice at one week by 50-70%, the histologic effects in the residual cells are minimal (31). In contrast, in human GISTs, imatinib induces profound histologic effects, including necrosis, decreased cellularity, and fibrosis, although the duration of treatment is much longer. However, tumor weight may not be a reliable measure of outcome for anti-CD40 and other therapies that may initially induce intratumoral inflammation and edema. Wolchok et al. established that response to immunotherapy may be better measured by immune-related response criteria compared to traditional assessment of treatment response (40), as immune cell infiltration into lesions may be inaccurately interpreted as progressive disease. Therefore, we utilized several other measurements to determine the antitumor effects of anti-CD40 and imatinib, including percentage of Kit^+ cells, tumor proliferation by Ki67 staining, treatment effect on H&E histology, and fibrosis by Trichrome staining.

We found that CD40 expression on a human GIST cell line was partially regulated by IFNγ, TNF, and TGFβ. Each of these cytokines was reduced in bulk $Kit^{V558\Delta/+}$ tumors by imatinib, and may be the cause of decreased tumor cell CD40 expression in $Kit^{V558\Delta/+}$ mice with imatinib.

Although anti-CD40 monotherapy in $Kit^{V558\Delta/+}$ mice stimulated TAMs (assessed by the expression of activation markers, cytokine production, and *in vitro* tumor cell killing), no detectable antitumor effects *in vivo* were observed. These findings imply that either the tumor microenvironment restrains activated macrophages or tumor cells are resistant to activated TAMs. We previously demonstrated in our mouse model that immunotherapy with either PD-1 or CTLA-4 blockade is not as effective without imatinib, in part, due to tumor production of IDO, which suppresses T cells (9, 11). It is likely that a similar immunosuppressive mechanism exists against TAMs, either through direct tumor-macrophage interaction or tumor cell factors. Imatinib reduces KIT signaling and tumor cell

proliferation, which are likely needed for antitumor TAM activity *in vivo*, as suggested by the inability of anti-CD40 and imatinib to exert an antitumor effect in an imatinib-resistant mouse model. The dependence of immunotherapy on imatinib in GIST is an important and recurrent theme.

The magnitude of the antitumor effects in $Kit^{V558\Delta/+}$ mice with established GISTs depended on the sequence of anti-CD40 and imatinib administration. When imatinib was started three days before anti-CD40 injection, TAMs were less activated and produced less TNF and IL6 four days later. Thus, imatinib modulated the tumor microenvironment (directly or via tumor cell inhibition) or TAMs to dampen TAM activation by anti-CD40. Our findings are consistent with those of Byrne et al., who found in a mouse model of pancreas cancer that hepatotoxicity occurs only when anti-CD40 is given prior to chemotherapy (41), indicating that an anti-CD40–induced effect is mitigated by chemotherapy. However, in that study, tumor inhibition was not affected by the sequence of therapy.

Lastly, we found that CD40 was expressed by TAMs and tumor cells in human GISTs, just like in our mouse model. No correlation between the expression of CD40 on tumor cells and TAMs was seen, suggesting that microenvironment factors, such as cytokine levels, do not fully dictate CD40 expression. However, expression was similar among different tumors from the same patient, suggesting that tumor intrinsic factors or host factors are responsible for the magnitude of CD40 expression. As in $Kit^{V558\Delta/+}$ mice, CD40 expression decreased with tyrosine kinase inhibition. CD40 expression was restored in patients who developed drug resistance, indicating that the effects of imatinib on CD40 expression were not direct but, rather, mediated via the inhibition of KIT signaling in tumor cells. Although CD40 expression did not correlate with location, mutation, or mitotic rate, a trend towards lower expression in wild-type GISTs was found, all of which were either untreated or resistant. Thus, CD40 expression appears to depend on the molecular pathogenesis of GIST, and anti-CD40 may not be indicated for certain GIST subtypes. In conclusion, CD40 is expressed in murine and human GIST, anti-CD40 improved upon the antitumor effects of imatinib therapy, and the mechanism depended largely on TAMs and partially on $CD8^+$ T cells. Therefore, combined treatment with anti-CD40 and imatinib has clinical potential for the treatment of GIST.

Supplementary Material

Refer to Web version on PubMed Central for supplementary material.

Acknowledgments

Financial support: The investigators were supported by NIH grants R01 CA102613 and T32 CA09501, Betsy Levine-Brown and Marc Brown, and David and Monica Gorin (RPD); GIST Cancer Research Fund (RPD and CRA); F32 CA186534 (JQZ); and P50 CA140146-01 (CRA). The Flow Cytometry and Molecular Cytology Core Facilities were supported by Cancer Center Support Grant P30 CA008748.

Acknowledgements

We are grateful to the Tissue Procurement Service for assistance in the acquisition of human tumor specimens. We thank members of the Sloan Kettering Institute Laboratory of Comparative Pathology, Molecular Cytology, Flow

Cytometry, and Pathology Core Facilities, Colony Management Group, and Research Animal Resource Center. We thank Russell Holmes for logistical and administrative support.

References

1. Joensuu H, DeMatteo RP. The management of gastrointestinal stromal tumors: a model for targeted and multidisciplinary therapy of malignancy. Annu Rev Med. 2012;63:247–58. [PubMed: 22017446]
2. Hirota S, Isozaki K, Moriyama Y, Hashimoto K, Nishida T, Ishiguro S, et al. Gain-of-function mutations of c-kit in human gastrointestinal stromal tumors. Science. 1998;279:577–80. [PubMed: 9438854]
3. Heinrich MC, Corless CL, Duensing A, McGreevey L, Chen CJ, Joseph N, et al. PDGFRA activating mutations in gastrointestinal stromal tumors. Science. 2003;299:708–10. [PubMed: 12522257]
4. Demetri GD, von Mehren M, Blanke CD, Van den Abbeele AD, Eisenberg B, Roberts PJ, et al. Efficacy and safety of imatinib mesylate in advanced gastrointestinal stromal tumors. N Engl J Med. 2002;347:472–80. [PubMed: 12181401]
5. Blanke CD, Rankin C, Demetri GD, Ryan CW, von Mehren M, Benjamin RS, et al. Phase III randomized, intergroup trial assessing imatinib mesylate at two dose levels in patients with unresectable or metastatic gastrointestinal stromal tumors expressing the kit receptor tyrosine kinase: S0033. Journal of clinical oncology : official journal of the American Society of Clinical Oncology. 2008;26:626–32. [PubMed: 18235122]
6. Verweij J, Casali PG, Zalcberg J, LeCesne A, Reichardt P, Blay JY, et al. Progression-free survival in gastrointestinal stromal tumours with high-dose imatinib: randomised trial. Lancet. 2004;364:1127–34. [PubMed: 15451219]
7. Demetri GD, Reichardt P, Kang YK, Blay JY, Rutkowski P, Gelderblom H, et al. Efficacy and safety of regorafenib for advanced gastrointestinal stromal tumours after failure of imatinib and sunitinib (GRID): an international, multicentre, randomised, placebo-controlled, phase 3 trial. Lancet. 2013;381:295–302. [PubMed: 23177515]
8. Demetri GD, van Oosterom AT, Garrett CR, Blackstein ME, Shah MH, Verweij J, et al. Efficacy and safety of sunitinib in patients with advanced gastrointestinal stromal tumour after failure of imatinib: a randomised controlled trial. Lancet. 2006;368:1329–38. [PubMed: 17046465]
9. Balachandran VP, Cavnar MJ, Zeng S, Bamboat ZM, Ocuin LM, Obaid H, et al. Imatinib potentiates antitumor T cell responses in gastrointestinal stromal tumor through the inhibition of Ido. Nature medicine. 2011;17:1094–100.
10. Cavnar MJ, Zeng S, Kim TS, Sorenson EC, Ocuin LM, Balachandran VP, et al. KIT oncogene inhibition drives intratumoral macrophage M2 polarization. The Journal of experimental medicine. 2013;210:2873–86. [PubMed: 24323358]
11. Seifert AM, Zeng S, Zhang JQ, Kim TS, Cohen NA, Beckman MJ, et al. PD-1/PD-L1 Blockade Enhances T-cell Activity and Antitumor Efficacy of Imatinib in Gastrointestinal Stromal Tumors. Clinical cancer research : an official journal of the American Association for Cancer Research. 2017;23:454–65. [PubMed: 27470968]
12. Clark EA, Yip TC, Ledbetter JA, Yukawa H, Kikutani H, Kishimoto T, et al. CDw40 and BLCa-specific monoclonal antibodies detect two distinct molecules which transmit progression signals to human B lymphocytes. Eur J Immunol. 1988;18:451–7. [PubMed: 2451615]
13. Ma DY, Clark EA. The role of CD40 and CD154/CD40L in dendritic cells. Semin Immunol. 2009;21:265–72. [PubMed: 19524453]
14. van Kooten C, Banchereau J. CD40-CD40 ligand. J Leukoc Biol. 2000;67:2–17. [PubMed: 10647992]
15. Schoenberger SP, Toes RE, van der Voort EI, Offringa R, Melief CJ. T-cell help for cytotoxic T lymphocytes is mediated by CD40-CD40L interactions. Nature. 1998;393:480–3. [PubMed: 9624005]
16. Diehl L, den Boer AT, Schoenberger SP, van der Voort EI, Schumacher TN, Melief CJ, et al. CD40 activation in vivo overcomes peptide-induced peripheral cytotoxic T-lymphocyte tolerance and augments anti-tumor vaccine efficacy. Nature medicine. 1999;5:774–9.

17. French RR, Chan HT, Tutt AL, Glennie MJ. CD40 antibody evokes a cytotoxic T-cell response that eradicates lymphoma and bypasses T-cell help. Nature medicine. 1999;5:548–53.
18. van Mierlo GJ, den Boer AT, Medema JP, van der Voort EI, Fransen MF, Offringa R, et al. CD40 stimulation leads to effective therapy of CD40(−) tumors through induction of strong systemic cytotoxic T lymphocyte immunity. Proceedings of the National Academy of Sciences of the United States of America. 2002;99:5561–6. [PubMed: 11929985]
19. Beatty GL, Chiorean EG, Fishman MP, Saboury B, Teitelbaum UR, Sun W, et al. CD40 agonists alter tumor stroma and show efficacy against pancreatic carcinoma in mice and humans. Science. 2011;331:1612–6. [PubMed: 21436454]
20. Jackaman C, Cornwall S, Graham PT, Nelson DJ. CD40-activated B cells contribute to mesothelioma tumor regression. Immunology and cell biology. 2011;89:255–67. [PubMed: 20628372]
21. Hess S, Engelmann H. A novel function of CD40: induction of cell death in transformed cells. The Journal of experimental medicine. 1996;183:159–67. [PubMed: 8551219]
22. Kalbasi A, Fonsatti E, Natali PG, Altomonte M, Bertocci E, Cutaia O, et al. CD40 expression by human melanocytic lesions and melanoma cell lines and direct CD40 targeting with the therapeutic anti-CD40 antibody CP-870,893. J Immunother. 2010;33:810–6. [PubMed: 20842056]
23. Tong AW, Papayoti MH, Netto G, Armstrong DT, Ordonez G, Lawson JM, et al. Growth-inhibitory effects of CD40 ligand (CD154) and its endogenous expression in human breast cancer. Clinical cancer research : an official journal of the American Association for Cancer Research. 2001;7:691–703. [PubMed: 11297266]
24. Vonderheide RH, Glennie MJ. Agonistic CD40 antibodies and cancer therapy. Clinical cancer research : an official journal of the American Association for Cancer Research. 2013;19:1035–43. [PubMed: 23460534]
25. Sommer G, Agosti V, Ehlers I, Rossi F, Corbacioglu S, Farkas J, et al. Gastrointestinal stromal tumors in a mouse model by targeted mutation of the Kit receptor tyrosine kinase. Proceedings of the National Academy of Sciences of the United States of America. 2003;100:6706–11. [PubMed: 12754375]
26. Bosbach B, Deshpande S, Rossi F, Shieh JH, Sommer G, de Stanchina E, et al. Imatinib resistance and microcytic erythrocytosis in a KitV558Delta;T669I/+ gatekeeper-mutant mouse model of gastrointestinal stromal tumor. Proceedings of the National Academy of Sciences of the United States of America. 2012;109:E2276–83. [PubMed: 22652566]
27. Cohen NA, Zeng S, Seifert AM, Kim TS, Sorenson EC, Greer JB, et al. Pharmacological Inhibition of KIT Activates MET Signaling in Gastrointestinal Stromal Tumors. Cancer research. 2015;75:2061–70. [PubMed: 25836719]
28. Taguchi T, Sonobe H, Toyonaga S, Yamasaki I, Shuin T, Takano A, et al. Conventional and molecular cytogenetic characterization of a new human cell line, GIST-T1, established from gastrointestinal stromal tumor. Laboratory investigation; a journal of technical methods and pathology. 2002;82:663–5. [PubMed: 12004007]
29. Ruifrok AC, Johnston DA. Quantification of histochemical staining by color deconvolution. Anal Quant Cytol Histol. 2001;23:291–9. [PubMed: 11531144]
30. DeNardo DG, Brennan DJ, Rexhepaj E, Ruffell B, Shiao SL, Madden SF, et al. Leukocyte complexity predicts breast cancer survival and functionally regulates response to chemotherapy. Cancer Discov. 2011;1:54–67. [PubMed: 22039576]
31. Kim TS, Cavnar MJ, Cohen NA, Sorenson EC, Greer JB, Seifert AM, et al. Increased KIT inhibition enhances therapeutic efficacy in gastrointestinal stromal tumor. Clinical cancer research : an official journal of the American Association for Cancer Research. 2014;20:2350–62. [PubMed: 24583793]
32. Van Rooijen N, Sanders A. Liposome mediated depletion of macrophages: mechanism of action, preparation of liposomes and applications. Journal of immunological methods. 1994;174:83–93. [PubMed: 8083541]
33. Elgueta R, Benson MJ, de Vries VC, Wasiuk A, Guo Y, Noelle RJ. Molecular mechanism and function of CD40/CD40L engagement in the immune system. Immunol Rev. 2009;229:152–72. [PubMed: 19426221]

34. Hoesel B, Schmid JA. The complexity of NF-kappaB signaling in inflammation and cancer. Molecular cancer. 2013;12:86. [PubMed: 23915189]

35. Hagemann T, Biswas SK, Lawrence T, Sica A, Lewis CE. Regulation of macrophage function in tumors: the multifaceted role of NF-kappaB. Blood. 2009;113:3139–46. [PubMed: 19171876]

36. Zitvogel L, Rusakiewicz S, Routy B, Ayyoub M, Kroemer G. Immunological off-target effects of imatinib. Nat Rev Clin Oncol. 2016;13:431–46. [PubMed: 27030078]

37. Isogawa M, Chung J, Murata Y, Kakimi K, Chisari FV. CD40 activation rescues antiviral CD8(+) T cells from PD-1-mediated exhaustion. PLoS Pathog. 2013;9:e1003490. [PubMed: 23853599]

38. Ngiow SF, Young A, Blake SJ, Hill GR, Yagita H, Teng MW, et al. Agonistic CD40 mAb-Driven IL12 Reverses Resistance to Anti-PD1 in a T-cell-Rich Tumor. Cancer research. 2016;76:6266–77. [PubMed: 27634762]

39. Zippelius A, Schreiner J, Herzig P, Muller P. Induced PD-L1 expression mediates acquired resistance to agonistic anti-CD40 treatment. Cancer Immunol Res. 2015;3:236–44. [PubMed: 25623164]

40. Wolchok JD, Hoos A, O'Day S, Weber JS, Hamid O, Lebbe C, et al. Guidelines for the evaluation of immune therapy activity in solid tumors: immune-related response criteria. Clinical cancer research : an official journal of the American Association for Cancer Research. 2009;15:7412–20. [PubMed: 19934295]

41. Byrne KT, Leisenring NH, Bajor DL, Vonderheide RH. CSF-1R-Dependent Lethal Hepatotoxicity When Agonistic CD40 Antibody Is Given before but Not after Chemotherapy. J Immunol. 2016;197:179–87. [PubMed: 27217585]

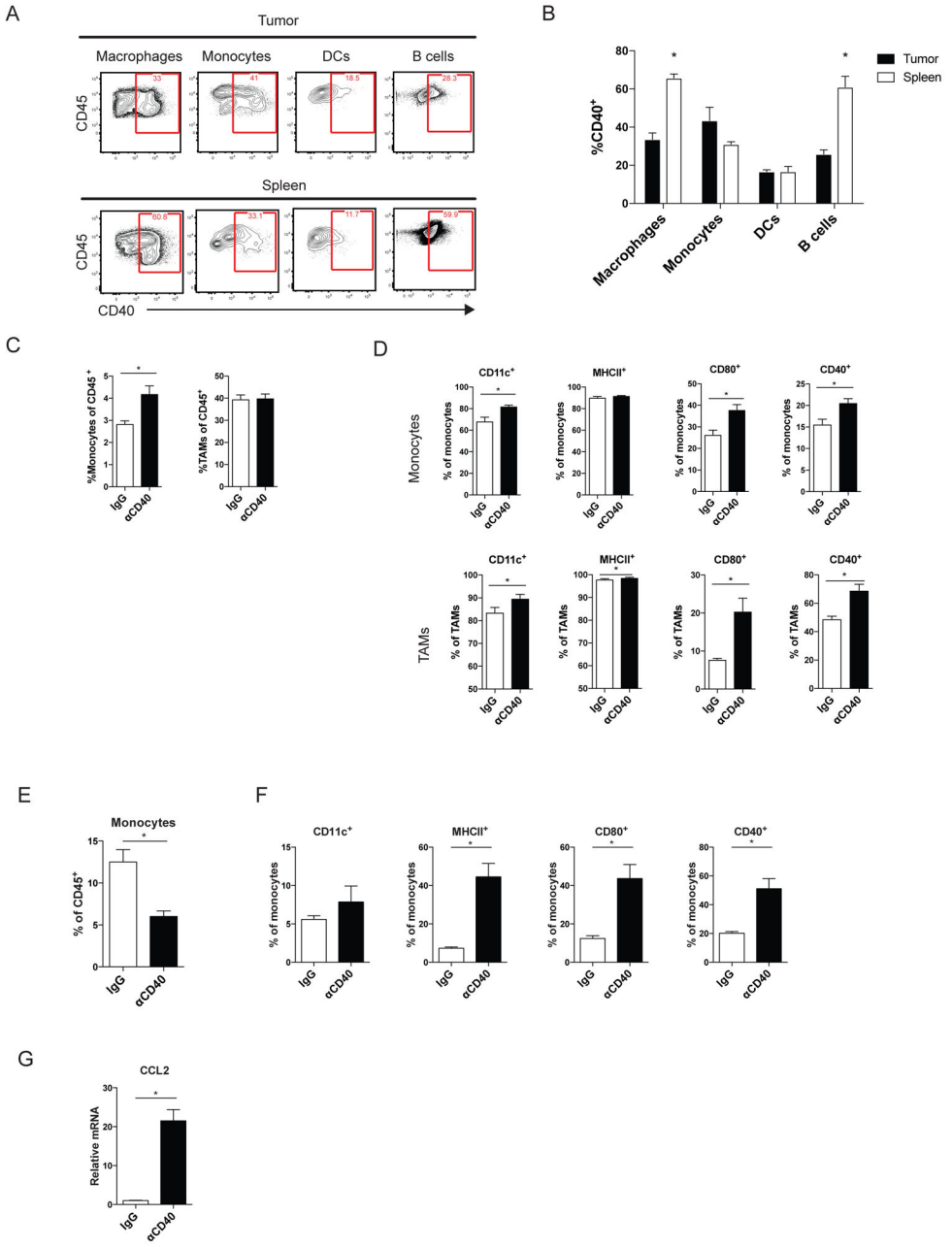

Figure 1. Anti-CD40 activates TAMs and recruits inflammatory monocytes.

(A) Representative flow plots of CD40 expression in the indicated cell types within an untreated tumor (top) and spleen (bottom). **(B)** Graph of $CD40^+$ cells as percentage of the indicated cell type in the tumor and spleen. $Kit^{V558\Delta/+}$ mice (5 mice/group) were treated for 3 days with anti-CD40 (αCD40) alone. **(C)** Intratumoral monocytes ($CD45^+Ly6G^-CD11b^+F4/80^+Ly6C^{hi}$) and TAMs ($CD45^+Ly6G^-CD11b^+F4/80^+Ly6C^{lo}$) were identified and assessed for **(D)** percentage of CD11c, MHCII, CD80, and CD40 expression. **(E)** Bone marrow (BM) monocytes ($Ly6C^+CD11b^+$) in $Kit^{V558\Delta/+}$ mice were identified 1 day after αCD40 alone (5 mice/group) and assessed for **(F)** percentage of CD11c, MHCII, CD80, and CD40 expression by flow cytometry. **(G)** CCL2 mRNA expression in bulk tumors from mice

1 day after αCD40. Data represent 1-5 experiments, mean ± SEM, *$P < 0.05$ using Student's *t* test.

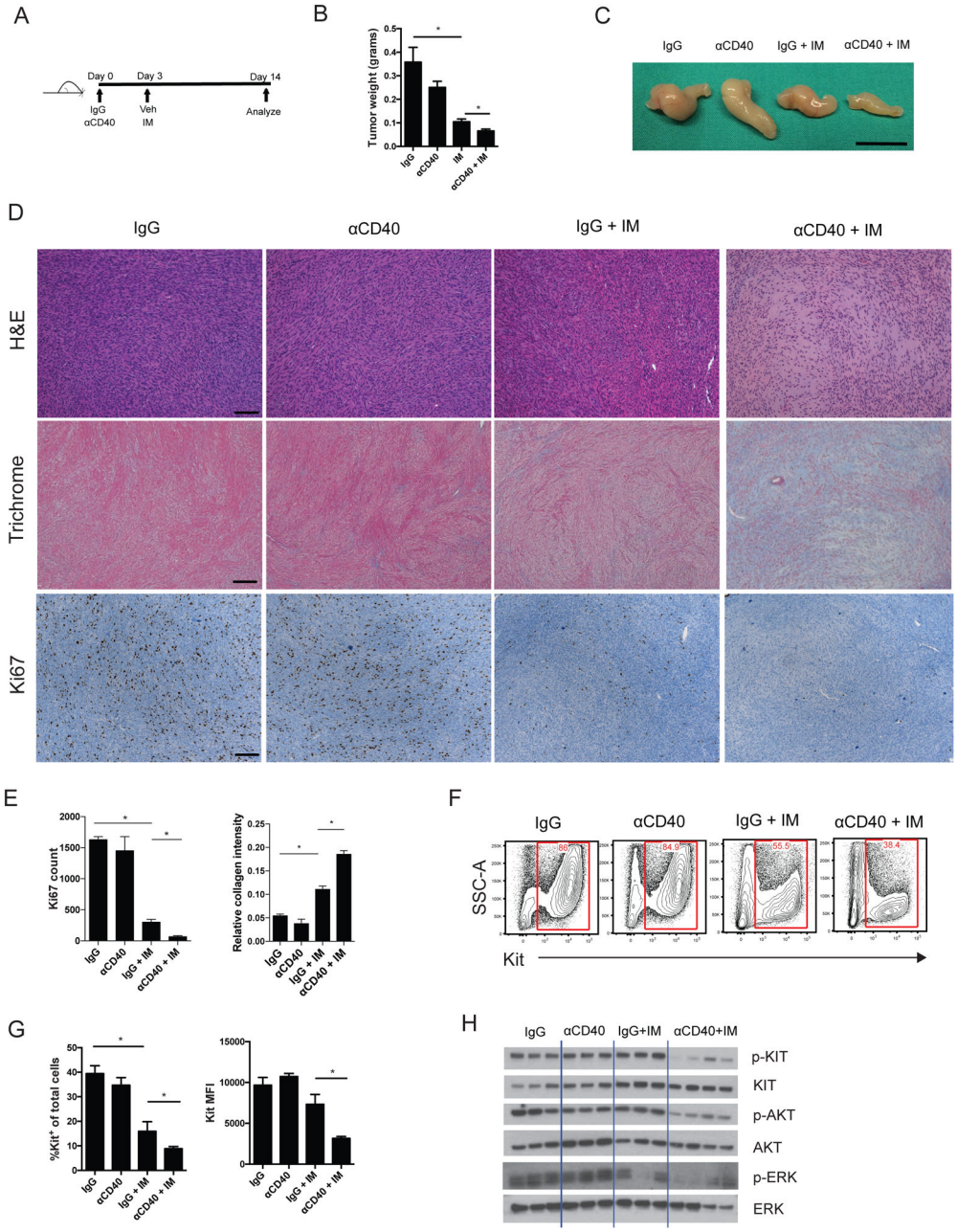

Figure 2. CD40 ligation increases the antitumoral effects of imatinib.

(A) Treatment schedule for combination therapy with anti-CD40 (αCD40) and imatinib (IM) in *Kit*$^{V558\Delta/+}$ mice, detailing a single injection of αCD40 on day 0, followed by continuous imatinib starting on day 3. All analyses were done after 2 weeks of treatment. 3-7 mice/group. **(B)** Tumor weight. **(C)** Photograph of representative tumors. Bar represents 1 cm. **(D)** Representative H&E, trichrome, and Ki67 staining of tumors. Bar represents 100 μm. **(E)** Ki67 count representing the number of positively stained nuclei in one 900 × 700 μm field per tumor (left) and collagen quantification by Trichrome staining (right). **(F)** Flow cytometry showing representative plots of Kit^{+} tumor cells (CD45^{-}Kit^{+}). **(G)** Flow cytometry assessment of percentage Kit-expressing cells and Kit mean fluorescence

intensity (MFI) of Kit^+ tumor cells. **(H)** Western blot for total and phosphorylated proteins. Data represent 3 experiments, mean ± SEM, $*P < 0.05$ using Student's *t* test.

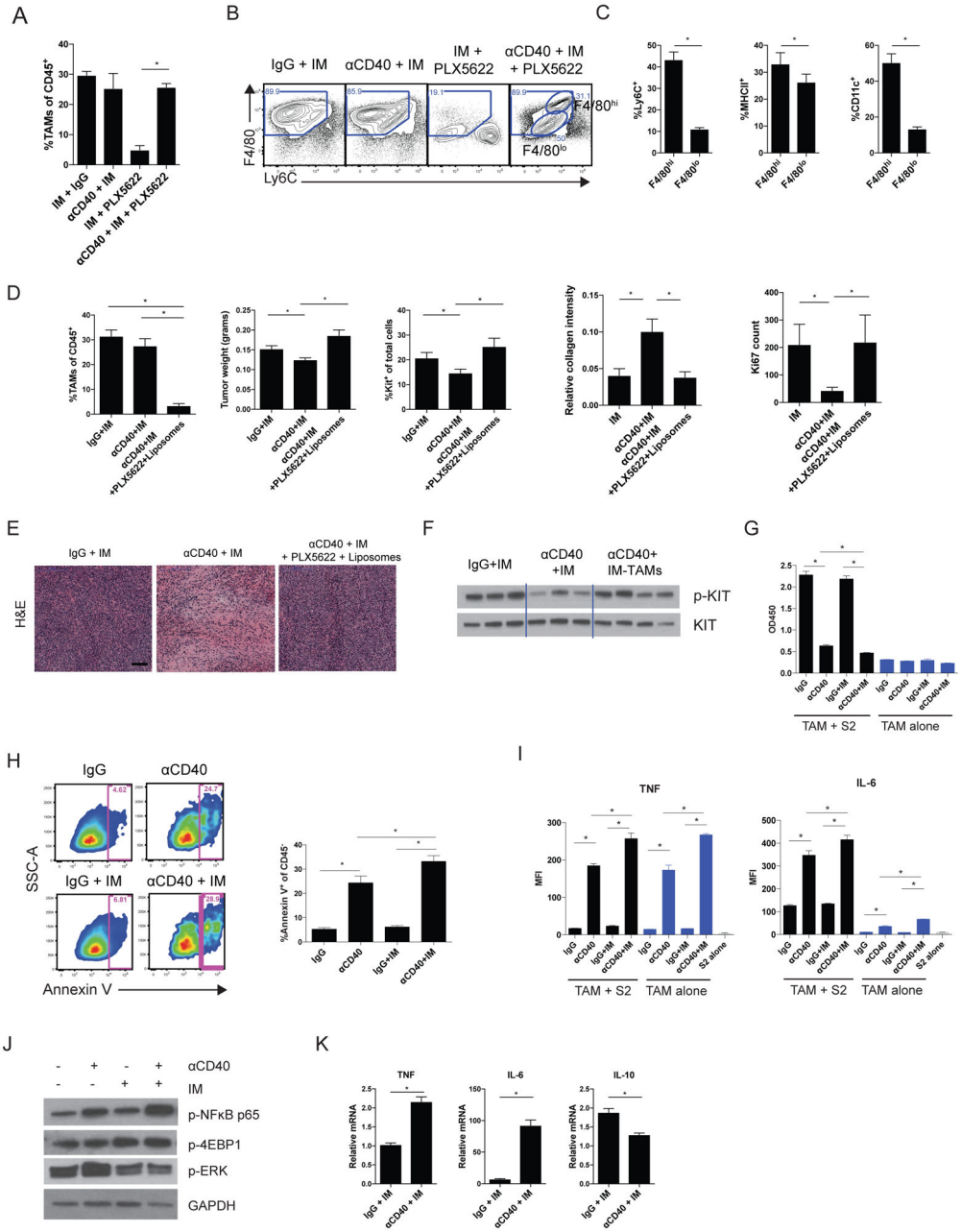

Figure 3. Anti-CD40 combination therapy is macrophage dependent.

(A) Percentage of TAMs 2 weeks after treatment, as indicated, and **(B)** representative flow plots (4-8 mice/group). **(C)** Ly6C, MHCII, and CD11c expression as percentage of F4/80^{hi} or F4/80^{lo} TAMs in mice treated with combination anti-CD40 (αCD40), imatinib (IM), and PLX5622. **(D)** Percentage of TAMs of CD45^{+} cells, tumor weight, percentage of Kit^{+} tumor cells, collagen staining by Trichrome, and Ki67 count representing the number of positively stained nuclei in one 800 × 720 μm field in *Kit*$^{V558Δ/+}$ mice depleted of TAMs (by PLX5622 and liposomes) at 2 weeks (4-10 mice/group). **(E)** Representative H&E tumor sections. Bar represents 100 μm. **(F)** Western blot of phospho-KIT in bulk tumors of *Kit*$^{V558Δ/+}$ mice depleted of TAMs. TAMs from *Kit*$^{V558Δ/+}$ mice treated *in vivo* for 4 days with a single

injection of αCD40 on day 0 and imatinib starting on day 3 or the corresponding controls (pooled from 3-4 mice) were plated in 96-well round-bottom plates, either alone or cocultured with the S2 tumor cell line for 3 days. **(G)** Cell viability was measured by optical density at 450 nm (OD450). **(H)** Representative flow plots of Annexin V staining of $CD45^-$ S2 tumor cells with corresponding bar graphs. Supernatants were harvested to measure **(I)** TNF and IL6 production with a cytometric bead array. **(J)** Western blot of TAMs isolated from $Kit^{V558\Delta/+}$ mice 4 days after treatment with αCD40 and imatinib. **(K)** Relative TNF, IL6, and IL10 mRNA of TAMs flow sorted from $Kit^{V558\Delta/+}$ mice 2 weeks after treatment. Data represent 2-3 experiments, mean ± SEM, $*P < 0.05$ using Student's *t* test.

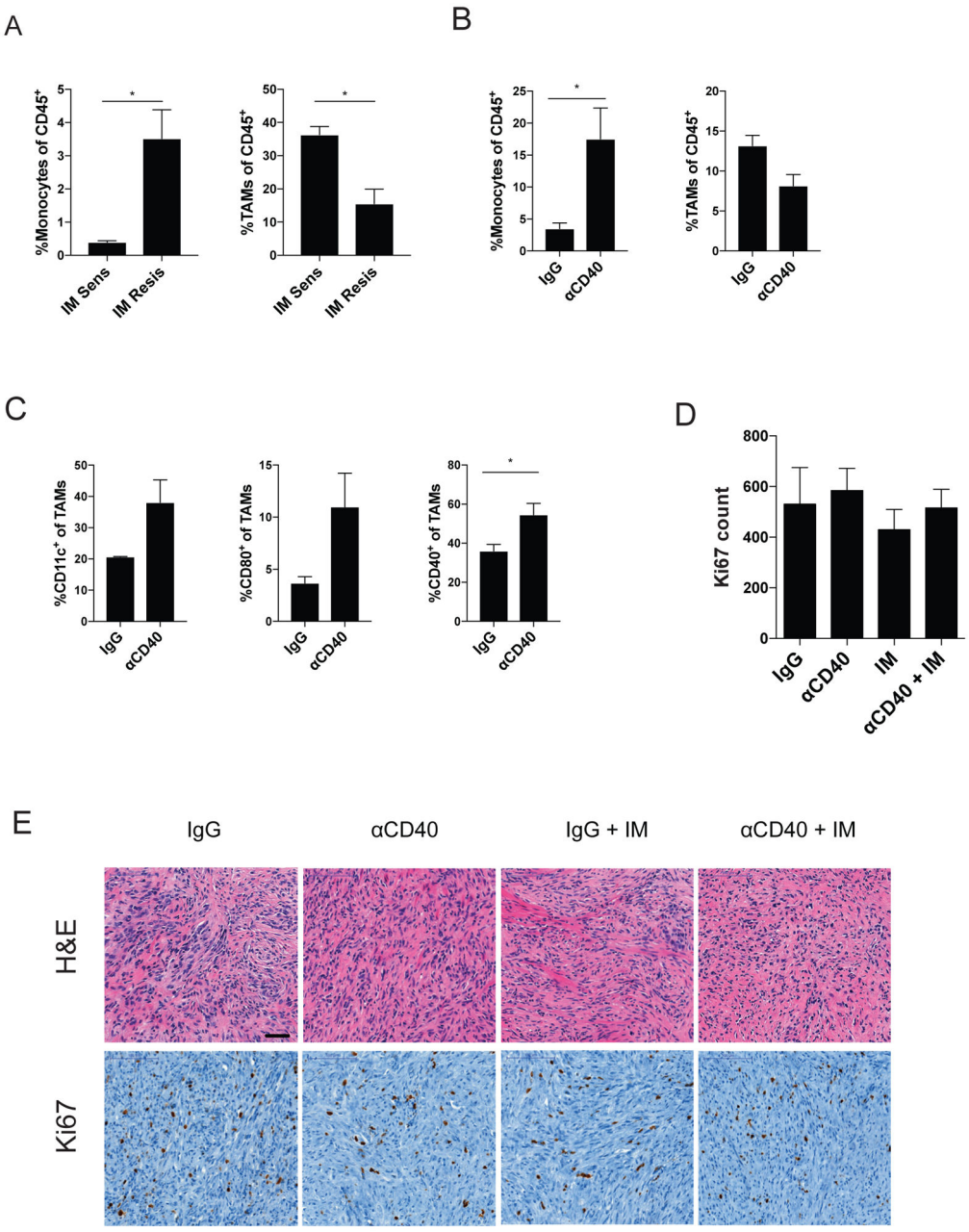

Figure 4. KIT inhibition may be needed for tumor response.

(A) Monocytes and TAMs, as a percentage of $CD45^+$ cells, in the imatinib (IM) sensitive ($Kit^{V558\Delta/+}$) and imatinib resistant ($Kit^{V558\Delta;T669I/+}$) tumors. $Kit^{V558\Delta;T669I/+}$ tumors were analyzed by flow cytometry 3 days after anti-CD40 (αCD40) and assessed for **(B)** intratumoral monocytes and TAMs, as a percentage of $CD45^+$ cells, and **(C)** TAMs were assayed for expression of CD11c, CD80, and CD40 expression. $Kit^{V558\Delta;T669I/+}$ mice were treated with a single αCD40 injection on day 0, followed by continuous imatinib on day 3. **(D)** Ki67 count representing the number of positively stained nuclei in one 800 × 730 μm field per tumor. **(E)** Representative H&E and Ki67 IHC. Bar represents 50 μm. Data represent 2 experiments, mean ± SEM, $*P < 0.05$ using Student's *t* test.

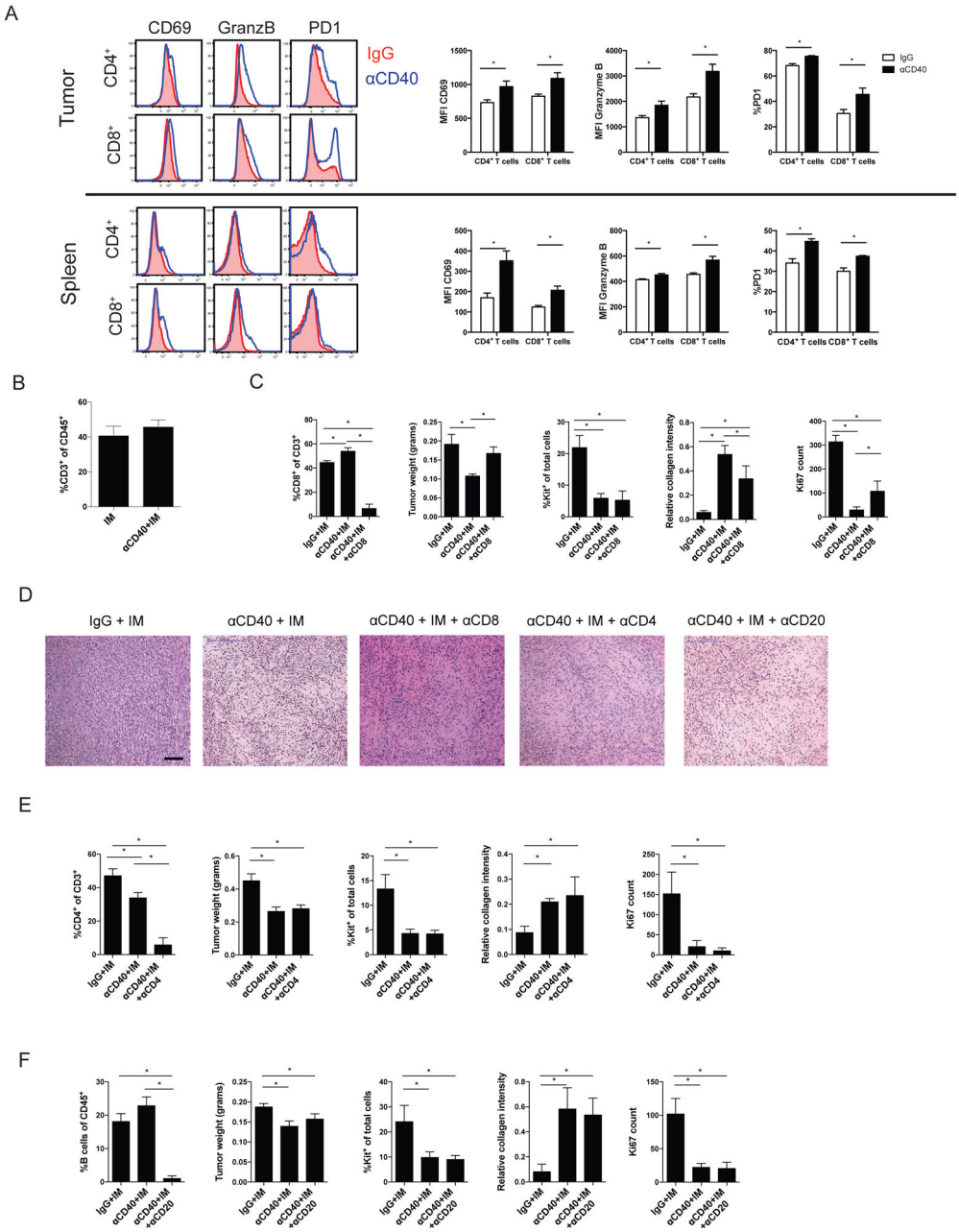

Figure 5. Anti-CD40 combination therapy is partially dependent on CD8$^+$ T cells.

(A) Left: Histograms of CD69, granzyme B (GranzB), and PD-1 expression on CD4$^+$ and CD8$^+$ T cells from the tumor (top) and spleen (bottom) of *Kit*$^{V558\Delta/+}$ mice (5–6 mice/group) 3 days after injection of IgG (red) or anti-CD40 (αCD40; blue). Right: Quantitation of results. MFI, mean fluorescence intensity. **(B)** CD3$^+$ T cells as percentage of CD45$^+$ cells in the tumor. **(C)** CD8$^+$ T cells as percentage of CD3$^+$ T cells in the tumor, tumor weight, Kit$^+$ tumor cells as percentage of total cells, collagen staining by Trichrome, and Ki67 count representing the number of positively stained nuclei in one 800 × 720 μm field in *Kit*$^{V558\Delta/+}$ mice at 2 weeks that were depleted of CD8$^+$ T cells and treated as indicated (7 mice/group). Imatinib: IM **(D)** Representative H&E tumor sections at 2 weeks. Bar represents 100 μm.

(E) $CD4^+$ T cells as percentage of $CD3^+$ T cells in the tumor, tumor weight, Kit^+ tumor cells as percentage of total cells, collagen staining by Trichrome, and Ki67 count representing the number of positively stained nuclei in one 600 × 600 μm field in $Kit^{V558\Delta/+}$ mice depleted of $CD4^+$ T cells at 2 weeks (3-5 mice/group). **(F)** B cells as percentage of $CD45^+$ cells, tumor weight and Kit^+ tumor cells as percentage of total cells, collagen staining by Trichrome, and Ki67 count representing the number of positively stained nuclei in one 600 × 600 μm field in $Kit^{V558\Delta/+}$ mice depleted of B cells at 2 weeks (6-7 mice/group). Data represent 2 experiments, mean ± SEM, $*P < 0.05$ using Student's *t* test.

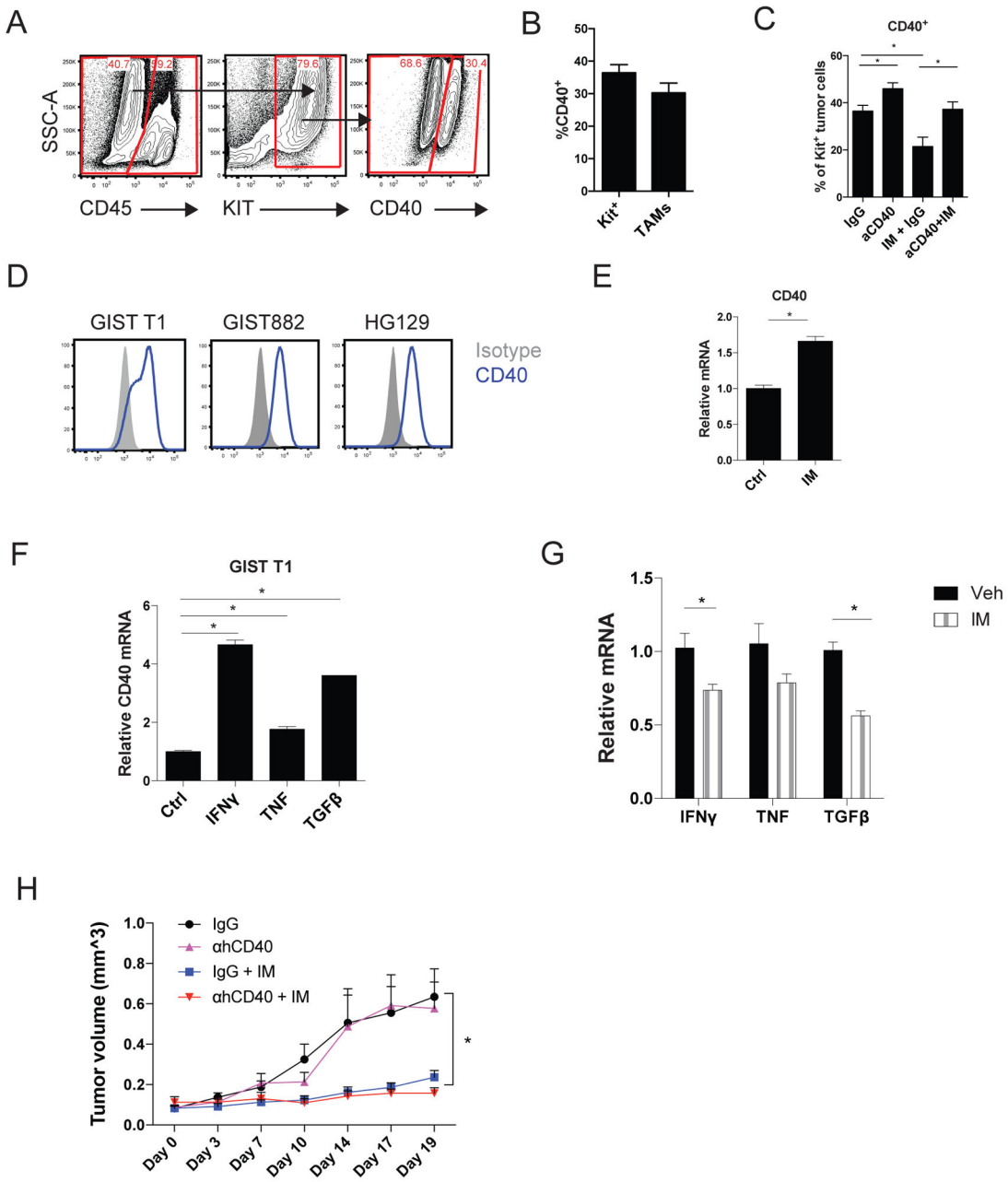

Figure 6. CD40 ligation does not directly inhibit GIST cells.

Untreated *Kit*$^{V558\Delta/+}$ mice (n=4) were analyzed for **(A)** CD40 expression on Kit^{+} tumor cells by flow cytometry and **(B)** CD40 expression was quantitated as a percent of Kit^{+} cells or TAMs. **(C)** CD40 expression as percent of Kit^{+} cells with the indicated treatment at 2 weeks (4-6 mice/group). Anti-CD40 (αCD40); Imatinib (IM). **(D)** CD40 expression by flow cytometry. **(E)** GIST T1 cells were treated *in vitro* for 8 hours, as indicated, and tested for relative CD40 mRNA levels. **(F)** GIST T1 cells were treated *in vitro* for 6 hours, as indicated, and tested for relative CD40 mRNA levels. **(G)** Relative IFNγ, TNF, and TGFβ mRNA expression in bulk tumor from *Kit*$^{V558\Delta/+}$ mice at 2 weeks. **(H)** Mice (5-6 mice/group) with established GIST T1 xenografts were injected once with anti-human CD40

followed by starting continuous imatinib 3 days later. Tumors were measured by calipers every 2-4 days. Treatments are as follows: IgG (black), anti-human CD40 (purple), IgG and imatinib (blue), anti-human CD40 and imatinib (red). Data represent mean ± SEM, $*P < 0.05$ using Student's *t* test.

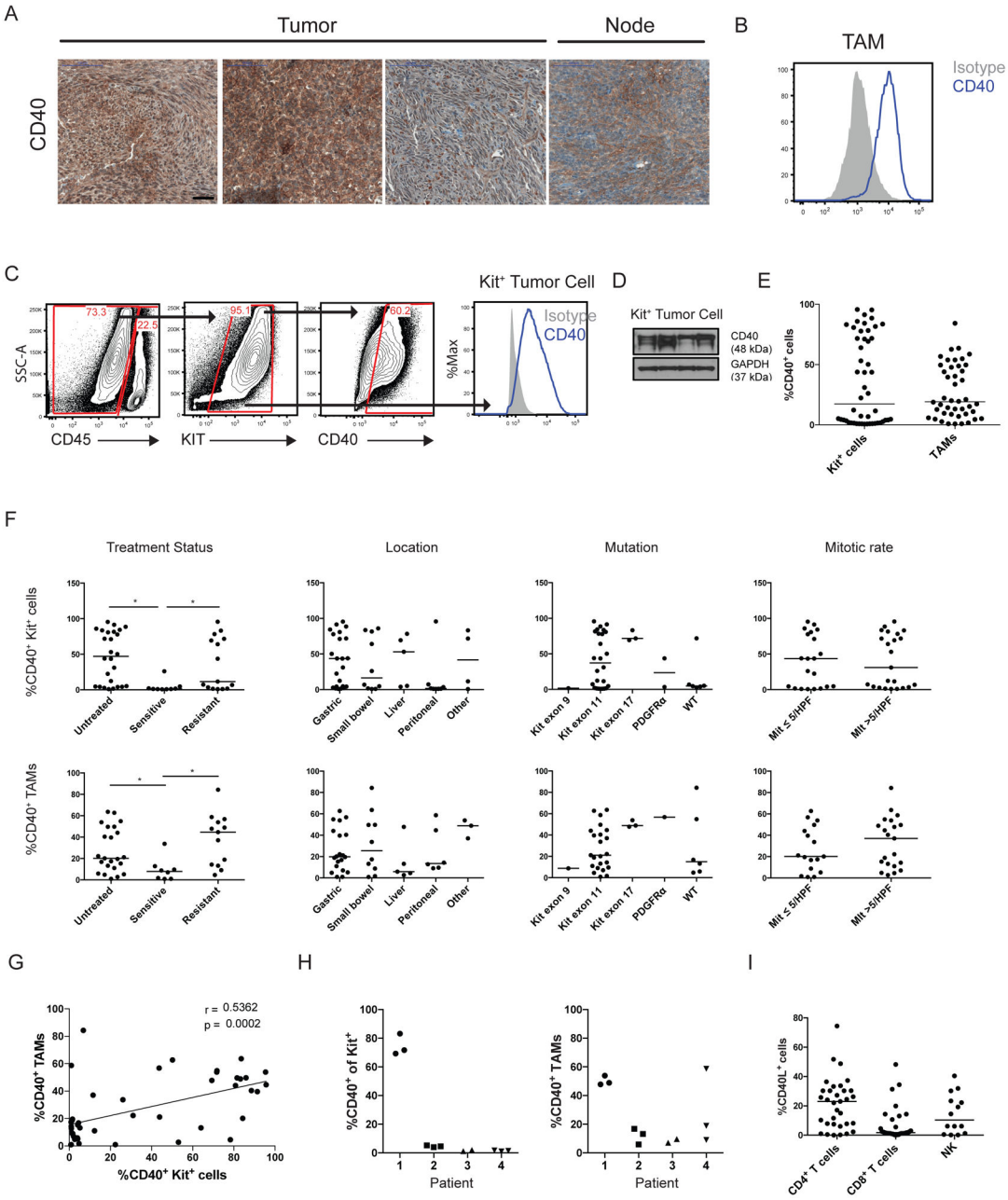

Figure 7. CD40 is expressed in human GISTs and correlates with treatment status.

(A) Representative CD40 staining in selected human GISTs, with lymph node (Node) as a positive control. Bar represents 50 μm. **(B)** Representative histogram of CD40 expression (blue) on human GIST TAMs by flow cytometry compared to isotype (gray). **(C)** Representative gating of $CD40^{+}Kit^{+}CD45^{-}$ tumor cells in human GIST (left) and histogram of CD40 expression (right, blue) on human Kit^{+} tumor cells by flow cytometry compared to isotype (gray). **(D)** Western blot of Kit^{+} tumor cells isolated from 4 separate human GIST specimens. **(E)** Dot plot of percentage of $CD40^{+}$ Kit^{+} tumor cells (n=50) and TAMs (n=44) by flow cytometry, and **(F)** the results were stratified by treatment status, location, mutation, and mitotic rate. “Untreated” tumors were from patients who never received a tyrosine

kinase inhibitor before surgery. “Sensitive” tumors were responding to imatinib or another tyrosine kinase inhibitor at the time of surgery. “Resistant” tumors were progressing despite treatment with imatinib or another tyrosine kinase inhibitor. **(G)** Spearman correlation of linear regression analysis comparing percentage of $CD40^+$ Kit^+ tumor cells and $CD40^+$ TAMs from individual human GISTs by flow cytometry. **(H)** Percentage of $CD40^+$ Kit^+ tumor cells (left) and TAMs (right) by flow cytometry among different tumors from the same patient (n=4). **(I)** Percentage of $CD40L^+$ T cells ($CD45^+CD3^+NK1.1^-$) and NK cells ($CD45^+CD3^-NK1.1^+$) within the tumor as assessed by flow cytometry. Bar represents median, $*P < 0.05$ using Student’s *t* test unless otherwise indicated.